

High performance and Current Drive Study on TRIAM-1M

ZUSHI Hideki*, ITOH Satoshi, SATO Kohnosuke, NAKAMURA Kazuo,
SAKAMOTO Mizuki, HANADA Kazuaki, JOTAKI Eriko, MAKINO Ken-ichi,
PAN Yudong¹, KAWASAKI Shoji, NAKASHIMA Hisatoshi
*Advanced Fusion Research Center, Research Institute for Applied Mechanics
Kyushu University, Kasuga, Fukuoka 816-8580, Japan*

(Received: 19 January 2000 / Accepted: 11 June 2000)

Abstract

A steady plasma with high performance and high current drive efficiency is reported. A new favorable regime is obtained in an 8.2 GHz LHCD plasma at high power (130–240 kW). Achieved plasma parameters are as follows; n_e is $4.3 \times 10^{13} \text{ cm}^{-3}$, I_{LHCD} is $\sim 70 \text{ kA}$, T_e and T_i are 0.8 keV and 0.5 keV, respectively, and the stored energy is 1.9 kJ. The energy confinement time τ_E of $\sim 8\text{--}10 \text{ ms}$ is achieved and the current drive efficiency $\eta_{CD} = n_e I_{CD} R_0 / P_{LH}$ reaches $\sim 1 \times 10^{19} \text{ A m}^2/\text{W}$ at $B = 7 \text{ T}$ under the full current drive condition. This regime characterized by improvement of both η_{CD} and τ_E is triggered by a transition when the power exceeds a certain threshold power.

Current control experiments have been performed by using two opposite traveling waves at 8.2 GHz. The current reduction ($\Delta I_{CD}/I_{CD} < -10\%$) is clearly seen when the backward traveling LHW ($\Delta\Phi = +90^\circ$) are added to a target plasma whose current is driven by forward traveling LHW ($\Delta\Phi = -90^\circ$). As the backward LHW power is increased, however, the current reduction becomes small and finally, it increases by a small amount ($\sim 10\%$) compared with the target plasma level. Mechanisms for this nonlinear behavior with respect to the backward LHW power will be discussed.

Keywords:

current drive, lower hybrid wave, tokamak

1. Introduction

It is well recognized that the steady state plasma is required to realize a nuclear fusion reactor. In the superconducting tokamak device TRIAM-1M [1] the proof-of-principle experiments for steady state tokamak (SST) operation have been successfully carried out. The discharge duration of more than two hours has been achieved by lower hybrid current drive (LHCD) technique at low power and low current level ($\sim 20 \text{ kW}$ and $\sim 30 \text{ kA}$) [2]. Recent our research activities for SST are on the following items: (1) realization of high performance plasma with an internal transport barrier, (2) establishment of the current profile controllability,

(3) understanding for effects of plasma surrounding components on steady state operation. It has been recognized that there are dominant timescales among the different physical processes, for example, energy and particle confinement times τ_E , τ_p for transport study, the current diffusion time $\tau_{L/R}$ for current profile control, and the recycling time $\tau_{recycling}$ for plasma-wall interaction. In order to advance the SST concept the combination of physical processes with different timescales should be investigated.

Two topics from recent SST research activities will be presented in this paper. The first topic relates to a new discharge mode (Enhanced Current Drive regime)

*Corresponding author's e-mail: zushi@triam.kyushu-u.ac.jp

¹On leave from Southwestern Institute of Physics, 610041, China.

characterized by simultaneously achievement of high current drive efficiency η_{CD} and improved energy confinement time. Achieved η_{CD} is by a factor of ~ 2.5 higher than the empirical scaling law based on JT-60 [3], and $H_{ITEP89-P}$ is ~ 1.4 [4]. The power dependence of ECD regime shows that there exists a threshold power range during which ECD is realized. The important time scale for which ECD regime is triggered will be discussed.

The second topic covers the results of the current profile control study. In order to achieve a hollow current density profile $j(r)$ we tested the combination of two LH waves traveling in the opposite directions. Especially to study the controllability of $j(r)$, backward (BW) traveling waves are injected into a LHCD plasma whose current is already driving by forward (FW) traveling LHW, that is, fast electrons are accelerated in the forward direction by FW waves.

This paper is conducted as follows. The brief description of the experimental conditions, LHCD systems and characteristics of LHW will be given in Sec. 2. The main aspects of the ECD regime will be presented in Sec. 3. The role of superposition of LHWs with opposite $N_{||}$ spectra on controllability of current profile will be reported in Sec. 4. Summary is given in Sec. 5.

2. Experimental Conditions, LHCD Systems and Characteristics of LHW

2.1 LHCD plasma and system hardware

In these experiments 8.2 GHz LHCD systems have been used. The configuration is the D-shaped poloidal

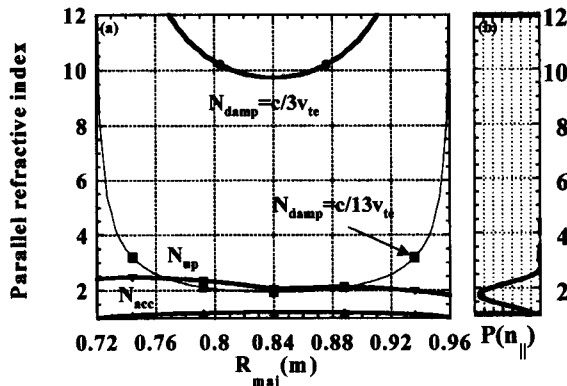


Fig.1 Characteristic parallel refractive indices, (a) N_{acc} , N_{up} , N_{damp} are plotted as a function of R_{maj} . $n_e(r)$ and $T_e(r)$ are parabolic, and squared parabolic $j(r)$ is used. (b) The launched $N_{||}$ spectrum is also shown.

limiter. The plasma minor radius a_p is ~ 0.12 m and the major radius R_0 is 0.84 m. The working gas is hydrogen. The direction of the toroidal magnetic field is clockwise viewing from the top of the machine and the direction of the driven current is also clockwise. In this case we call forward current drive by forward traveling LHW. When the direction of the wave vector is reversed, backward-traveling LHW is launched.

Two sets of the 8.2 GHz system having 8 klystrons of 25 kW each are separated toroidally by 180° . The grill type of antenna is used and the antenna phasing $\Delta\Phi$ is also scanned by the phase shifter from 70° to 270° , but most data are taken at 90° , whose peak parallel refractive index N_{peak} is ~ 1.65 corresponding to resonant electron energy of 100 keV.

2.2 Characteristics of LHW

For 8.2 GHz LHW there is no lower hybrid resonance point because of $B_0 \leq 8$ T. Under these experimental conditions the ratio of the LHW frequency to the calculated lower hybrid resonance frequency is 4–10.

The launched LHW can penetrate into the whole region because of high B_t and high frequency. The critical refractive index N_{acc} (bottom line) does not affect the wave propagation, because $N_{peak} > N_{acc}$ [5]. The up-shifting of LHW refractive index N_{up} (second thick line from the bottom) is caused by the toroidal effects, but the maximum value of N_{up} is limited ~ 2 , because of high aspect ratio of 7 and high q ($=13$) operation. Thus the phase velocity of the up-shifting wave is about 13 times larger than the electron thermal velocity v_{te} ($N_{damp} \sim c/13v_{te}$). In this sense there exists a large 'spectral gap' between them [6].

3. ECD Regime

A new operation regime, ECD, is found in high power 8.2 GHz LHCD plasmas. The record values of plasma performance obtained in the ECD regime are η_{CD} of $0.9\text{--}1 \times 10^{19}$ Am²/W and τ_E of 8–10 ms, respectively. The driven current is 70 kA and the density is 4.3×10^{13} cm⁻³. Total plasma energy including the high energy component reaches ~ 2 kJ at launched rf power of 230 kW. The ion and electron temperatures are 0.5 keV and 0.9 keV, respectively.

As mentioned in Sec. 1, the ECD regime is characterized by both improvement of η_{CD} and τ_E . The obtained η_{CD} is compared with the empirical scaling law, $\eta_{CD} = 12 \langle T_e \rangle / (5 + Z_{eff})$ [3], where $\langle T_e \rangle$ and Z_{eff} are a volume averaged electron temperature and effective

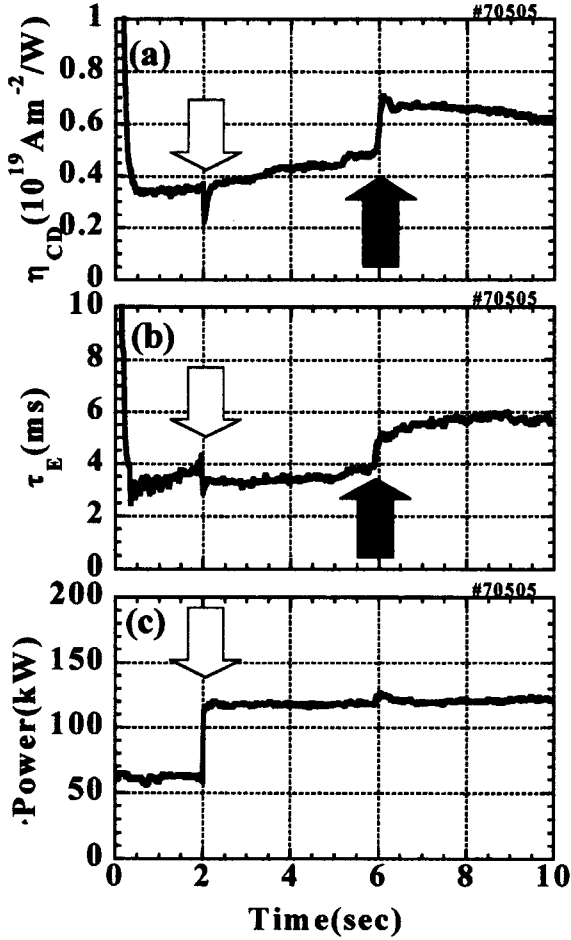


Fig. 2 (a) η_{CD} , (b) τ_E and (c) rf power are plotted as a function of time. P_{LH} is increased at 2 sec from 60 kW to 120 kW and then is kept constant. ECD occurred at ~ 6 sec.

charge, respectively. In ECD case the numerical factor is by 2.5 higher than this scaling with an assumption of $Z_{eff} = 1$. The theoretical explanation for this empirical scaling law has been reported [7,8], which is based on an enhancement of bridge from the thermal electrons to the resonant electrons. Although the spectral gap is very wide, the T_e increment from 0.5 keV to 0.9 keV in ECD contributes to the enhancement of η_{CD} . The confinement time is also compared with the ITER-89-P scaling [4] and H-factor of 1.4 is obtained. Phenomenological comparison with H-mode transition [9] will be given latter.

It is found that one of the necessary conditions for ECD to be realized is the LHCD power, that is, there exists a threshold power. Figure 2 shows one example obtained near the lower limit of the threshold power $P_{threshold}$. At $t = 2$ sec P_{LH} is increased from 60 kW to

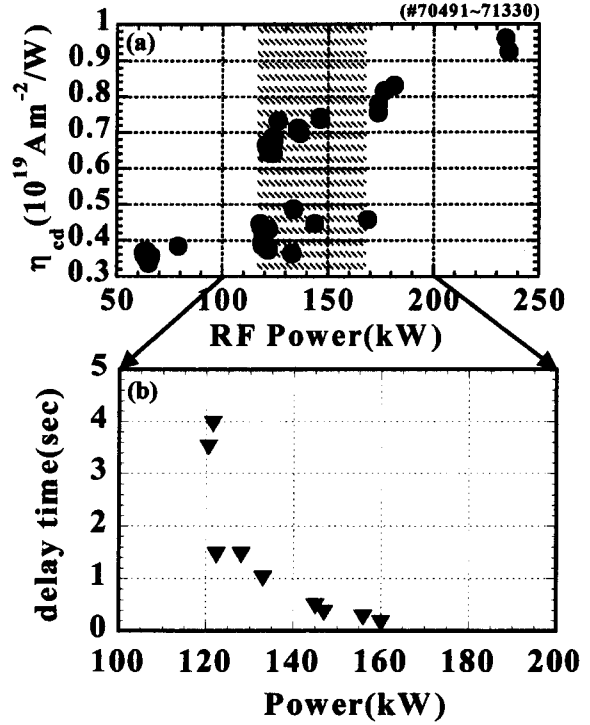


Fig. 3 (a) η_{CD} versus P_{LH} . In the hatched area plasma has two values of η_{CD} during a pulse width. (b) τ_{delay} decreases with increasing P_{LH} .

120 kW. Although both I_{LHCD} and n_e are increased by 40% – 50%, no enhancement of both η_{CD} and τ_E are observed. After that P_{LH} is kept constant in time. The ECD event occurs with a delay time τ_{delay} of ~ 4 sec. Although the improved factors are not high because of the lower power, clear jumps of both η_{CD} and τ_E , denoted by filled arrows in Fig. 2, are observed under the constant power level. We consider that during τ_{delay} hidden parameters may grow with a very long time constant. In this discharge τ_{LR} is 0.1–0.2 sec, therefore the necessary delay time for ECD to be triggered is at least several tens of τ_{LR} at the lowest threshold power.

The power dependence of ECD phenomenon is carefully studied to obtain the range of the variation of $P_{threshold}$ and also to get a power dependence of τ_{delay} , as shown in Fig. 3. The target plasma is sustained by LHW at fixed power of 85 kW. Additional LHW is injected 2 seconds after the plasma is initiated. Thus the target plasma parameters for additional LHW injection are kept constant. The power level of the additional LHW is varied shot by shot and the power dependence of τ_{delay} is obtained. We observe that ECD occurs within a range of $P_{threshold}$ (120 kW–170 kW), which means $\Delta P_{threshold} / \langle P_{threshold} \rangle$ is 30%. Here, $\Delta P_{threshold}$ is the power window,

hatched region in Fig. 3, and $\langle P_{threshold} \rangle$ is the mean value of the threshold power. It is also found that τ_{delay} becomes short and finally it approaches to 0.18 sec ($\sim \tau_{L/R}$) as P_{LH} increases up to ~ 170 kW, which is the upper limit of $P_{threshold}$. Above this value it is expected that the transition for ECD may occur with a shorter time constant. These experiments are left for future. This threshold power level is almost 1/3 compared with the ITER H-mode power scaling [10]. This reduced value may depend on τ_{delay} , which is not taken into account for the H-mode power threshold database. In order to reduce the threshold power above which an improved plasma state can be attained we must investigate the background physics for a relation between τ_{delay} and $P_{threshold}$.

A hysteresis of η_{CD} with respect to P_{LH} is found. In this experiment the power of one LHCD system is kept constant to sustain the performance of the target plasma and the power of the another one is varied in time for 6 sec from 0 kW to 85 kW and 85 kW to 0 kW. A relation, similar to one shown in Fig. 3, is observed around $P_{threshold}$ in a single shot. For case of power ramp-up η_{CD} jumps from 0.4 to 0.6×10^{19} Am²/W at around 155 kW and for case of power ramp-down it drops from 0.6 to 0.35×10^{19} Am²/W at 130 kW. We consider that this hysteresis is attributed to τ_{delay} for the ECD regime depending on the power [11].

In order to find triggering parameters, which dominate ECD event, several signals (I_{LHCD} , H_{α} density, charge exchange flux Φ_{cx} , ion saturation current I_{sat} in the scrape off layer) at the onset time of ECD are studied in detail. The reference time is defined as the time at which I_{LHCD} starts to increase. Within 1–2 ms H_{α} starts to decrease. The density rise is delayed by ~ 10 ms. The enhancement of n_e/H_{α} ratio suggests the improvement of the particle confinement in ECD. The reduction of I_{sat} also supports this. On the contrary Φ_{cx} enhances in spite of reduced H_{α} , suggesting Ti increase and better ion confinement. The change in Φ_{cx} precedes by ~ 30 ms with respect to the ECD event. Thus it is found that the fastest signal is Φ_{cx} . Although perpendicular Φ_{cx} measured along the major radius is sensitive to the formation of radial electric field E_r under some conditions [12], direct E_r measurement has been not yet performed. The order of these timescales is observed to be in the range of a few to several times τ_E . Thus within the fastest timescale (1–10) $\times \tau_E$ performance change of plasma is finished.

4. Current profile control experiments

It is widely recognized that a hollow current profile is necessary to improve the transport [13]. In order to get a hollow $j(r)$ we carried out the current profile control experiment by combining LHW ($\Delta\phi = \pm 90^\circ$) whose $N_{||}$ spectra are opposite, as shown in Fig. 4.

If both power spectra are the same, no driven current is expected in ideal case without the toroidal electric field because of the symmetric velocity distribution function along the parallel velocity. Since plasma current is already driven by forward LHW in this experiment, the change in the already flowing current is studied by applying backward LHW. The direction of the forward current is clockwise. The BW traveling LHW are injected into this target plasma. The antenna phasing are mainly -90° (FW) and $+90^\circ$ (BW), respectively, but the effect of BW $\Delta\phi$ on I_{LHCD} is also studied from $+70^\circ$ to $+180^\circ$. The power of BW-LHW is varied from 20 kW to 60 kW step by step and is kept constant for the injection duration (usually 2 sec).

The plasma parameters in this experiment are as follows: $n_e \sim 1.5 \times 10^{13}$ cm⁻³, $T_e(0) \sim 0.3$ keV and $T_i(0) \sim 0.2$ keV. The bulk plasma parameters are slightly changed when the BW-LHW are injected. The line density is reduced by $\sim 5\%$, but the power dependence of Δn_e is not significant. T_i is not changed or slightly (10–20 eV) decreased. Although T_e shows a large scattering, it is not concluded that electrons are heated by BW LHW within error bars. The change in the stored energy is from 0.3 to 0.4 kJ but τ_E is reduced from 3.5 ms to 2.2–2.7 ms. It is considered that the increment of the stored energy is attributed to the energetic electrons produced by BW LHW.

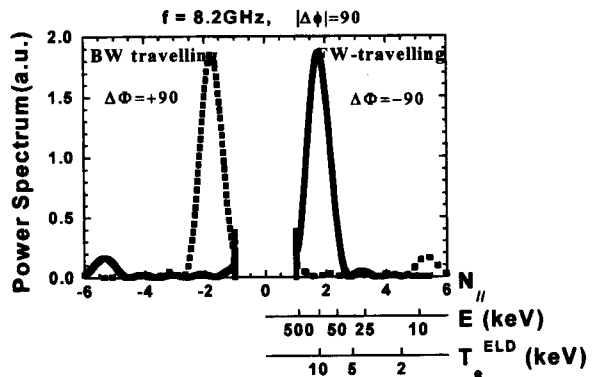


Fig. 4 The spectra for forward and backward traveling LHW whose antenna phasing are $\pm 90^\circ$. The peak parallel refractive index corresponds to the resonant energy of ~ 100 keV.

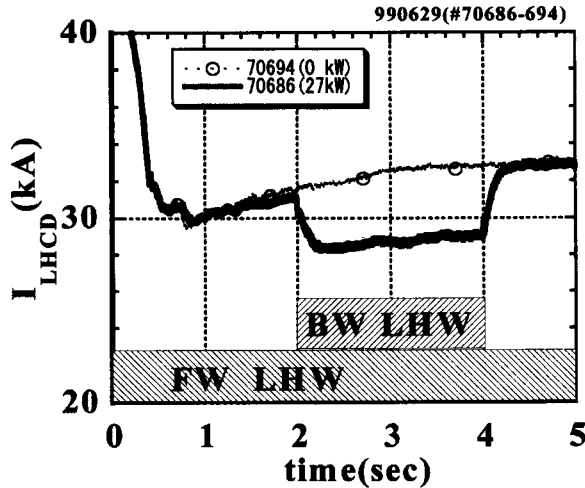


Fig. 5 I_{LHCD} is plotted as a function of time. The power sequence is shown in the figure. BW LHW are injected from 2 sec to 4 sec.

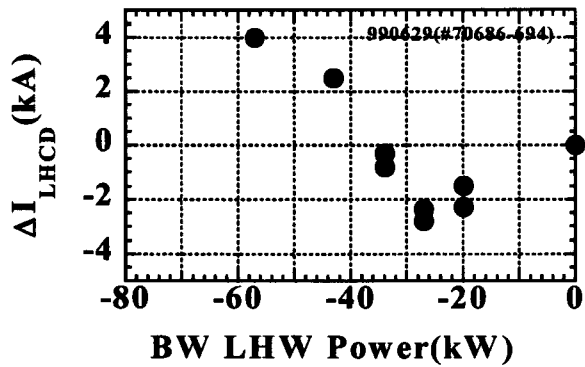


Fig. 6 The relative change in I_{LHCD} is plotted as a function of BW LHW.

We observe that the total current is clearly reduced when the BW-LHW are injected at low power, as shown in Fig. 5.

In this case BW LHW (~27 kW) are injected from 2 to 4 s. First the current dropped at the very beginning phase of BW injection and then it saturated within 0.2 sec. The toroidal electric field (< 100 mV) is produced during this transient phase. With increasing power the total current is reduced further, and the reduced value and the relative reduction factor reach -2 kA and -10% , respectively. When the BW power is increased above 27 kW, the further current reduction is suppressed, and then above ~ 34 kW the direction of the total driven current is completely reversed, that is, the direction becomes the same as that driven by FW-LHW. This power dependence of ΔI_{LHCD} is summarized in

Fig. 6.

Thus it should be noted that there are two phases, current compensation phase and enhanced forward current drive phase. Data points in this figure were taken at the middle of the pulse width as the typical mean values. However, in the early phase within 0.2 sec just after BW LHW was injected I_{LHCD} dropped by almost the same value and then it varied depending on its BW power during the rest of the pulse width. Thus current compensation by BW-LHW shows a highly nonlinear behavior with respect to the BW power.

In order to investigate controllability of $j(r)$ by BW LHW second experiment has been performed. The current profile change is monitored by Shafranov $\Lambda (= \beta_p + l_i/2 - 1)$ as a function of the BW power. Here β_p is poloidal beta and l_i is the internal inductance. In this experiment the BW power is varied smoothly in time from 5 to ~ 70 kW for 3 s. The similar results with respect to $\Delta I_{LHCD} - P_{BW}$ relation (shown in Fig. 6) are obtained in a single shot. During the current is compensated by BW LHW, Λ is monotonically increased and $\Delta \Lambda$ is ~ 0.8 . From this measurement and diamagnetism measurement the current profile becomes peaking during the current compensation phase. A drastic reduction is observed in Λ when the power is increased above the certain value (in this case ~ 40 kW). Since the hard X ray measurement does not change at this critical power level, the contribution of the energetic electrons to β_p is not so large. Thus at that power level $j(r)$ is changed from a peaked one to a broad one and then the broad profile is kept during the enhanced forward current drive phase. Finally the total current is increased higher than that in the initial FW LHCD plasma.

Although the observed counter current drive scenario shows a nonlinear behavior depending on the current compensating BW power, the following explanations are considered for the current compensation process. In order to interact for BW LHW with resonant electrons moving in the clockwise direction, energetic trapped electrons produced via pitch angle scattering process may be necessary. There are two situations with respect to the confinement time τ_{fast} of the energetic electrons. In order to satisfy the condition $\tau_{fast} > \tau_{sc}$ (scattering time) the order of 0.2 sec of τ_{fast} is necessary. If the large angle scattering process occurs, these trapped electrons are directly created. These electrons are drifting in back and forth directions along their fat banana orbits, that is, when they are drifting in the BW-direction, resonant interaction occurs

between BW-LHW and these trapped electrons. This results in detrapping the barely trapped energetic electrons drifting in the backward direction, and therefore, the backward current is produced [14]. Thus the total current $I_{tot} = I_{FW} - I_{BW}$ is reduced. Since trapped particles are located in the outer board, the in-out asymmetry in hard X ray profile is responsible for this mechanism. Since backward current tends to flow in the outer region and current cancellation is expected there, the final current density profile will become peaked. This is supported by enhancement of l_i . The plausible theoretical explanations for the second enhanced FW current drive phase are given in ref. [15,16] based on the large angle scattering process and small toroidal electric field effects. Quantitative comparison with these theories is left in the future.

5. Summary

In summary the high performance and current profile control experiments in LHCD plasmas are described.

The ECD regime is obtained in high power 8.2 GHz LHCD plasmas and it is found that there exists the threshold power level for the ECD regime to be triggered. This regime is characterized by simultaneous improvement of η_{CD} and τ_E .

In order to aim at compensating the current and obtaining a hollow profile the current profile control experiment is carried out by using two opposite traveling LHWs. The backward traveling waves are injected into target plasma whose current is already driven by forward traveling waves. The results show a non-linear response in the change of the driven current as the backward wave power is increased.

References

- [1] S. Itoh *et al.*, in Plasma Phys. Control. Nucl. Fusion Research 1986 (Proc. 11th Int. Conf., Kyoto, 1986) Vol. 3, IAEA Vienna, 321 (1987).
- [2] S. Itoh *et al.*, in Fusion Energy 1996 (Proc. 16th Int. Conf., Montreal, 1996) Vol. 3, IAEA, Vienna, 351 (1997).
- [3] Y. Ikeda *et al.*, in 15th IAEA Conf. Plasma Phys. and Contr. N. F. Res. Vol. 1, 415 (1994).
- [4] P.N. Yushmanov *et al.*, Nucl. Fusion **30**, 1999 (1990).
- [5] T.H. Stix, 1992 Chapter 4 in 'Waves in Plasmas', American Institute of Physics New York.
- [6] N.J. Fisch, Rev. of Mod. Phys. **59**, 175-234 (1987).
- [7] K. Ushigusa, Plasma Phys. and Control. Fusion **38**, 1825-1830 (1996).
- [8] E. Barbato, Plasma Phys. and Control. Fusion **40**, A63-A76 (1998).
- [9] F. Wagner *et al.*, Phys. Rev. Lett. **49**, 1408 (1982).
- [10] K. Thomsen *et al.*, in 17th IAEA Int. Conf. on Fusion Energy 1998, Yokohama, IAEA-CN-69/ITERP1/07.
- [11] H. Zushi *et al.*, Nuclear Fusion **40**, 1183 (2000).
- [12] J.A. Heikkinen, T. Kurki-Suonio and W. Herrmann, Plasma Phys. Control. Fusion **40**, 679 (1998).
- [13] D. Moreau and I. Voitsekhovitch, Nucl. Fusion **39**, 685-693 (1999).
- [14] T. Ohkawa, General Atomic Company Report GA-A 13847 (1976).
- [15] R. Jayakumar *et al.*, Phys. Lett. A **172**, 447-451 (1993).
- [16] V.S. Chan *et al.*, J. Plasma Fusion Res., *in press*.